Electronic Supplementary Material (ESI) for Catalysis Science & Technology.

Supporting Information

Title: Mechanistic Insights into CoO_x–Ag/CeO_2 Catalysts for the Aerobic Oxidation of 5-Hydroxymethylfurfural to 2,5-Furandicarboxylic Acid

Authors: Mengchen Fu[a], Weiyao Yang[a], Chenyu Yang[a], Yiwen Zhang[a], Chun Shen[a,b,*]

Affiliations:

[a]Beijing Key Laboratory of Bioprocess, College of Life Science and Technology, Beijing University of Chemical Technology, No. 15 of North Three-Ring East Road, Chaoyang District, Beijing 100029, P.R. China

[b]The State Key Laboratory of Chemical Engineering, Department of Chemical Engineering, Tsinghua University, Beijing 100084, P.R. China.

Numbers of pages: 10

Number of figures: 4

Number of tables: 9

Number of equations: 7

Corresponding authors:

Email address: shenchun@mail.buct.edu.cn (Chun Shen)

Preparation of Catalyst: Ag/CeO_2 and CoO_x–Ag/CeO_2-X (X represents the molar ratio of Co/Ag) catalysts were prepared by a hydrothermal method as described in related literature. Typically, 3.472 g of $Ce(NO_3)_3\cdot 6H_2O$ and 0.379 g $AgNO_3$ were dissolved in 20 mL of deionized water. The solution of 39.2 g NaOH was gradually added in the above solution. After stirring at room temperature for 30 min, the mixture was transferred into a Teflon-lined autoclave (100 mL) and treated at 100 °C for 24 h. The obtained solid was separated by centrifugation, washed with deionized water and ethanol several times, then dried at 80 °C in air overnight and calcined at 350 °C for 4 h in air with a heating rate of 4 °C min^{-1}. Then the as-formed catalyst was treated at 300 °C for 2 h in 10% H_2/N_2 stream (v/v) with a heating rate of 2 °C min^{-1}, then added to 100 mL of deionized water with 1 mL hydrazine hydrate in the solution and stirred for 30 min at 70 °C. The solid was taken out of solution and calcined at 400 °C for 4 h in air with a heating rate of 2 °C min^{-1}, and finally treated at 150 °C for 30 min in 10% H_2/N_2 stream (v/v) with a heating rate of 2 °C min^{-1} to obtain the Ag/CeO_2 catalysts. To prepare CoO_x–Ag/CeO_2-X (X represents the molar ratio of Co/Ag), the same method was used, with the desired amounts of $Co(NO_3)_2\cdot 6H_2O$ in the solution of hydrazine hydrate.

Ag/CeO_2-red was prepared by the method same as Ag/CeO_2, only without the step after the stirring for 30 min at 70 °C. CoO_x/CeO_2 (the molar ratio of Co/Ag was set as 2) catalyst was prepared by a method similar as Ag/CeO_2 catalysts. Typically, 3.472 g of $Ce(NO_3)_3\cdot 6H_2O$ was dissolved in 20 mL of deionized water. The solution of 39.2 g NaOH was gradually added in the above solution. After stirring at room temperature for 30 min, the mixture was transferred into a Teflon-lined autoclave (100 mL) and treated at 100 °C for 24 h. The obtained solid was separated by centrifugation, washed with deionized water and ethanol several times, then dried at 80 °C in air overnight and calcined at 350 °C for 4 h in air with a heating rate of 4 °C min^{-1}. Then the as-formed catalyst was treated at 300 °C for 2 h in 10% H_2/N_2 stream (v/v) with a heating rate of 2 °C min^{-1}, added to 100 mL of deionized water with 1 mL hydrazine hydrate and 1.29 g of $Co(NO_3)_2\cdot 6H_2O$ in the solution and stirred for 30 min at 70 °C. The solid was taken out of solution and calcined at 400 °C for 4 h in air with a heating rate of 2 °C min^{-1}, and finally treated at 150 °C for 30 min in 10% H_2/N_2 stream (v/v) with a heating rate of 2 °C min^{-1} to obtain CoO_x/CeO_2.

Catalyst Characterization: XRD patterns of reduced catalyst samples were measured on a Rigaku D/max 2500 diffractometer in 2θ range of 20–90°, with a scanning rate of 1°/min. XPS was measured using an Esca Lab 250Xi photoelectron spectrometer, and the binding energies were calibrated to the position of the C1s peak at 284.8 eV. Transmission electron microscope (TEM) images were obtained on a JEOL JEM-2011 high resolution transmission electron microscope at an operating voltage of 300 kV equipped with an EDS detector. The chemical compositions were determined using a NexION 1000 (ICP). The H_2-TPR and O_2-TPO were performed on Chemisorb 2720 (Micrometrics) equipped with a thermal conductive detector. The catalyst sample was pretreated in flowing He at 600 °C for 1 h. After the sample temperature drops to room temperature, the gas was switched to 10 vol% H_2/Ar or 10 vol% O_2/He (25 mL/min). After the baseline went smoothly, the sample was heated to 900 °C with a rate of 10 °C/min. O_2-TPD was also performed on Chemisorb 2720, after the same pretreatment process, the corresponding gas were switched to 10 vol% O_2/He. After saturated, the flowing gas were switched to the corresponding inert gas. After the baseline is stable, the sample was heated to 950 °C with a rate of 10 °C min^{-1}. The electron paramagnetic resonance (EPR) signals of spin-trapped radicals were recorded on a Bruker EMX-6/1 spectrometer to detect the active oxygen species in the reaction system. The ESR and Raman spectra is probed right after the full preparation, and the condition of ESR is similar to the reaction described below.

Catalyst Evaluation: The oxidation reaction of HMF was performed at 130 °C in a 50 mL high-pressure automatic stirring stainless-steel reactor. Under normal circumstances, the autoclave was loaded with 0.5 mmol HMF, 20 mL H_2O, 2 mmol NaOH and 0.3 g catalyst. Pure oxygen was purged three times to exclude the air in the autoclave, then the reactor was purged with O_2 with the pressure of 2 MPa, and the temperature was raised to 130 °C and the timing was started at a stirring speed of 600 rpm. After the reaction, the reactor was placed in an ice water bath, and then the solid-liquid mixture was centrifuged, and the liquid was filtered through a 0.45-micron organic membrane to remove impurities. The products were analyzed using high-performance liquid chromatography (HPLC, Shimadzu UFLC-XR) with an Aminex HPX-87H column and a UV detector. The column temperature was 30 °C, and the mobile phase was H_2SO_4 solution (5 mmol/L) with a flow rate of 0.5 mL/min. The detection wavelengths were 280 nm for HMF and FFCA, and 254 nm for HMFCA and FDCA. The conversion of HMF (X_{HMF}), the yield (Y_{P}), and selectivity (S_{P}) are calculated as follows:

(1)

$$Y_{\mathrm{P}}\ （\% = \frac{C_{\mathrm{P}}}{C_{\mathrm{HMF,initial}}} \times 100 \qquad (2)$$

$$S_{\mathrm{P}}(\%) = \frac{Y_{\mathrm{P}}}{X_{\mathrm{HMF}}} = \frac{C_{\mathrm{P}}}{C_{\mathrm{HMF,initial}} - C_{\mathrm{HMF,finial}}} \times 100 \qquad (3)$$

where C represents the concentrations of different components of the reaction system.

The reaction kinetic model: The consumption and generation rates of each substance are shown in Eqs. (4−7), where k_i represents the rate constant of each step and C_i represents the concentration of each substance.

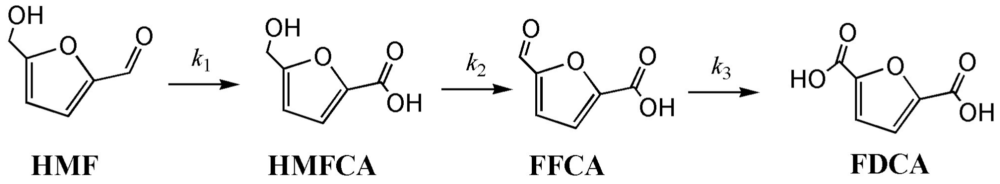

$$\frac{dC_{\mathrm{HMF}}}{dt} = -k_1 C_{\mathrm{HMF}} \tag{4}$$

$$\frac{dC_{\mathrm{HMFCA}}}{dt} = k_1 C_{\mathrm{HMF}} - k_2 C_{\mathrm{HMFCA}} \tag{5}$$

$$\frac{dC_{\mathrm{FFCA}}}{dt} = k_2 C_{\mathrm{HMFCA}} - k_3 C_{\mathrm{FFCA}} \tag{6}$$

$$\frac{dC_{\mathrm{FDCA}}}{dt} = k_3 C_{\mathrm{FFCA}} \tag{7}$$

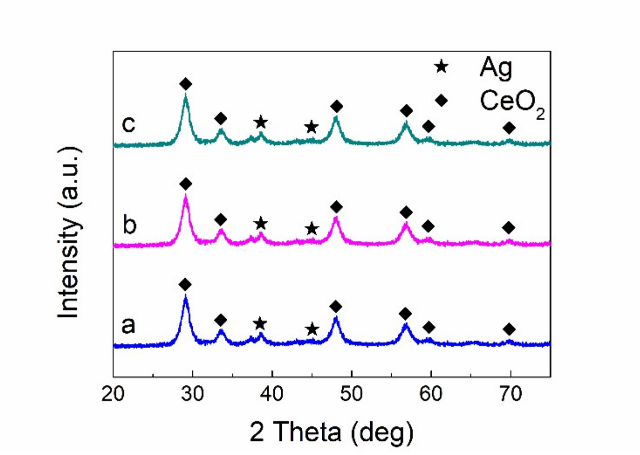

Fig. S1 XRD patterns of the catalysts; (a) CoO_x−Ag/CeO_2-1, (b) CoO_x−Ag/CeO_2-3, (c) CoO_x−Ag/CeO_2-4.

Table S1 Chemical Compositions of Prepared Catalysts from ICP Analyses.

Catalysts	Ag [wt%]	Co [wt%]
Ag/CeO_2	8.19	/
CoO_x−Ag/CeO_2-1	7.92	4.29
CoO_x−Ag/CeO_2-2	8.04	5.03
CoO_x−Ag/CeO_2-3	7.85	5.76
CoO_x−Ag/CeO_2-4	7.93	6.38

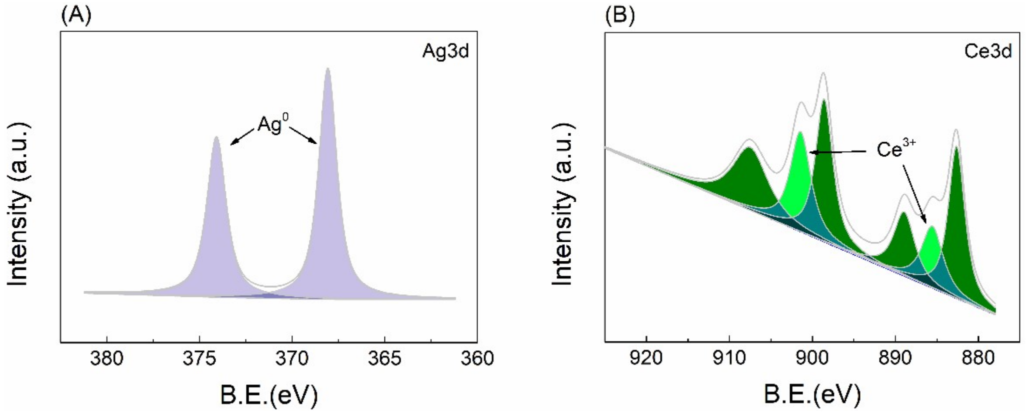

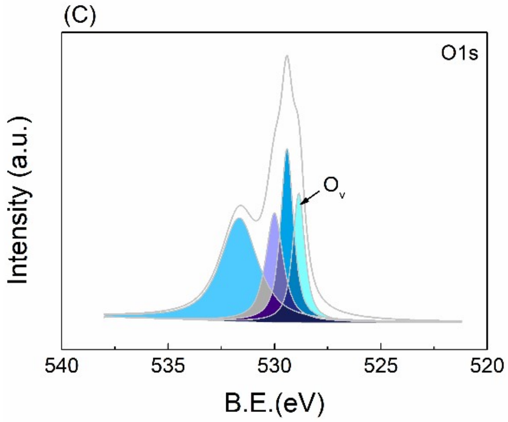

Fig. S2 XPS spectra of Ag/CeO$_2$-red. (A) Ag 3d, (B) Ce 3d, (C) O 1s.

Table S2 Proportion of Active Sites of Catalysts.

Catalysts	$Ag^+/(Ag^++Ag^0)$ [%]	$Ce^{3+}/(Ce^{3+}+Ce^{4+})$ [%]	O$_v$ concentration [%]	$Co^{2+}/(Co^{2+}+Co^{3+})$ [%]
Ag/CeO$_2$	31.6	34.2	10.4	/
CoO$_x$–Ag/CeO$_2$-1	62.5	34.9	14.5	51.7
CoO$_x$–Ag/CeO$_2$-2	74.7	35.7	49.3	52.4
CoO$_x$–Ag/CeO$_2$-3	71.8	35.1	18.8	52.0
CoO$_x$–Ag/CeO$_2$-4	55.9	34.3	12.1	51.5
Ag/CeO$_2$-red	0	27.7	8.8	/

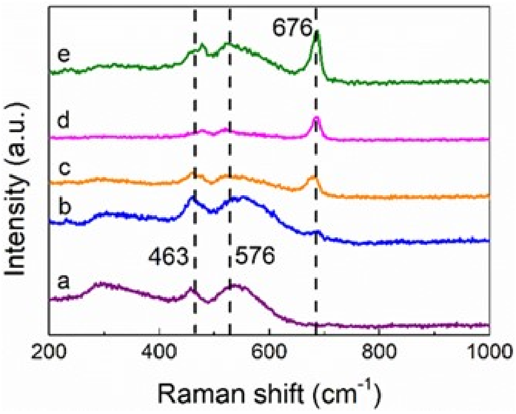

Fig.S3 Raman spectra of catalysts at 200–1000 cm^{-1}. (a) Ag/CeO$_2$, (b) CoO$_x$–Ag/CeO$_2$-1, (c) CoO$_x$–Ag/CeO$_2$-2, (d) CoO$_x$–Ag/CeO$_2$-3, (e) CoO$_x$–Ag/CeO$_2$-4.

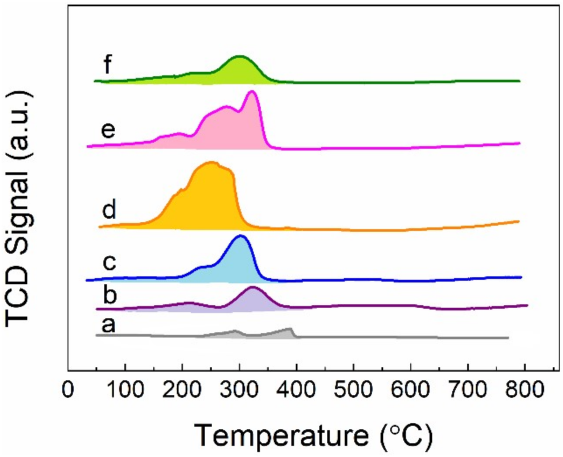

Fig. S4 H_2-TPR patterns of the catalysts. (a) Ag/CeO_2, (b) CoO_x−Ag/CeO_2-1, (c) CoO_x−Ag/CeO_2-2, (d) CoO_x−Ag/CeO_2-3, (e) CoO_x−Ag/CeO_2-4.

Table S3 Surface oxygen reducibility According to H2-TPR Profiles.

Samples	H_2 consumption [μmol/g]
CeO_2	12.7
Ag/CeO_2	21.9
CoO_x−Ag/CeO_2-1	54.4
CoO_x−Ag/CeO_2-2	125.4
CoO_x−Ag/CeO_2-3	97.7
CoO_x−Ag/CeO_2-4	39.4

Table S4 Oxidation of HMF over Ag-based catalyst in our work and previous work.

Entry	Catalyst	Base [eq.]	Conv (HMF) [%]	Yield (HMFCA) [%]	Yield (DFF) [%]	Yield (FDCA) [%]	Ref.
1	CoO_x−Ag/CeO_2-2	NaOH (4 eq)	100	-	-	93	This work
2	Ag-OMS-2	Base free	99	-	99	0	20
3	Ag_2O	Na_2CO_3 (4 eq)	100	98	-	0	21
4	Ag/ZrO_2	NaOH (4	100	92	-	5	22

		eq)					
5	Ag/CeO_2	NaOH (4 eq)	100	74	-	3	22
6	Ag/MgO	NaOH (4 eq)	100	60	-	1	22
7	Ag/TiO_2	NaOH (4 eq)	100	14	-	3	22
8	Ag_9Au_1/ZrO_2	NaOH (4 eq)	100	83	-	7	23
9	Ag-PVP/ZrO_2(1:1)	NaOH (4 eq)	100	98	-	0	24

Table S5 Oxidation of HMF with varied concentration and types of bases. [a]

NaOH of varied concentration	FDCA yield [%]	Different types of bases (4 eq)	FDCA yield [%]
8 eq	92.8	NaOH	92.8
4 eq	92.8	Na_2CO_3	88.4
2 eq	89.3	$NaHCO_3$	83.7

[a] Reaction conditions: HMF (0.5 mmol), catalyst (0.3 g), H_2O (20 mL), O_2 (2 MPa), 720 min.

Table S6 Catalytic test results of varied preparation methods. [a]

Preparation methods of CoO_x-Ag/CeO_2	FDCA yield [%]
hydrothermal	92.8
deposition-precipitation	69.7
wetness impregnation	66.3

[a] Reaction conditions: HMF (0.5 mmol), catalyst (0.3 g), NaOH (2 mmol), H_2O (20 mL), O_2 (2 MPa), 720 min.

Table S7 Catalytic test results of CoO_x/CeO_2 and Ag/CeO_2-red.[a]

Catalysts	HMF conversion [%]	FDCA yield [%]
CoO_x/CeO_2	100	24.2

Ag/CeO$_2$-red	100	6.9

[a] Reaction conditions: HMF (0.5 mmol), catalyst (0.3 g), NaOH (2 mmol), H_2O (20 mL), O_2 (2 MPa), 720 min.

Table S8 Catalyst reusability study for HMF oxidation.[a]

Catalysts reused	HMF Conversion [%]	FDCA yield [%]
1st run	100	92.8
2nd run	100	91.5
3rd run	100	90.6
4th run	100	90.8
5th run	100	90.1

[a] Reaction conditions: HMF (0.5 mmol), catalyst (0.3 g), NaOH (2 mmol), H_2O (20 mL), O_2 (2 MPa), 720 min.

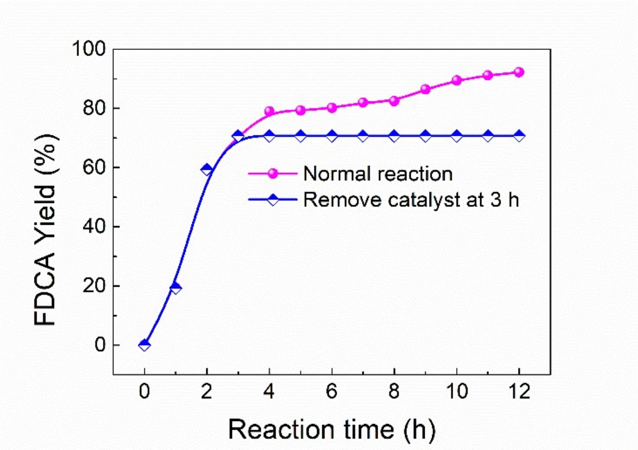

Fig.S5 Catalyst leaching test. Reaction conditions: HMF (0.5 mmol), catalyst (0.3 g), NaOH (2 mmol), H_2O (20 mL), O_2 (2 MPa), 720 min.

Table S9 TON of HMF Oxidation over Au-based catalyst and Ag-based catalyst in our work and previous work.

Entry	Catalyst	TON [mmol/h]	Ref.
1	CoO$_x$–Ag/CeO$_2$-2	6.00	This work
2	Ag-OMS-2	2.51	1
3	Ag$_2$O	0.75	2
4	Ag/ZrO$_2$	3.05	3
5	Ag/CeO$_2$	1.79	3

6	Ag/MgO	1.53	3
7	Ag/TiO_2	1.79	3
8	Ag_9Au_1/ZrO_2	4.00	4
9	$Ag\text{-}PVP/ZrO_2$(1:1)	1.98	5
10	Au/GC	115.63	6
11	$Au\text{-}CeO_2$	150.00	7
12	Au/CeO_2-rod	174.00	8
13	$Au/Ce_{1-x}Bi_xO_{2-\delta}$	149.93	9
14	Au/MgO	123.50	10
15	Au/Al_2O_3	119.76	11
16	Au/ZrO_2	125.00	12
17	Au/HT	145.83	13
18	$Au/Ce_xZr_{1-x}O_2$	100.00	14

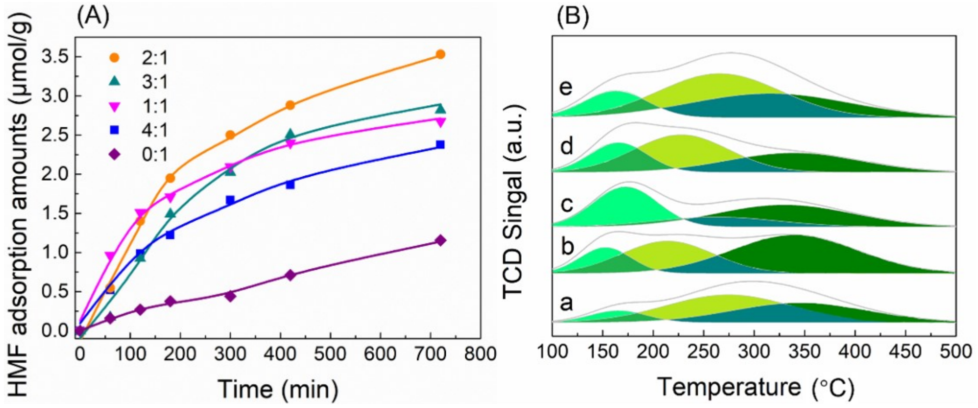

Fig.S6 (A) Adsorption curves of HMF and (B) O_2-TPD patterns of the catalysts. (a) Ag/CeO_2, (b) $CoO_x{-}Ag/CeO_2$-1, (c) $CoO_x{-}Ag/CeO_2$-2, (d) $CoO_x{-}Ag/CeO_2$-3, (e) $CoO_x{-}Ag/CeO_2$-4.

Table S10 Oxygen Adsorption Capacity According to O_2-TPD Profiles.

Catalysts	O_2 adsorption capacity [μmol/g]	O_{sur} / (O_{sur} + O_{lat} + O_{Bul}) ratio [%]
Ag/CeO_2	57.6	10.4
$CoO_x{-}Ag/CeO_2$-1	98.4	12.5
$CoO_x{-}Ag/CeO_2$-2	194.8	34.3

CoO_x−Ag/CeO_2-3	134.5	19.8
CoO_x−Ag/CeO_2-4	114.3	12.5

Table S11 Kinetic Parameters of HMF Oxidation on Ag/CeO_2 and CoO_x−Ag/CeO_2-*X* Catalysts.

Catalysts	Rate constant [min^{-1}]		
	k_1 (HMF → HMFCA)	k_2 (HMFCA → FFCA)	k_3 (FFCA → FDCA)
Ag/CeO_2	2.39	0.14	8.89
CoO_x−Ag/CeO_2-1	5.07	0.17	1.70
CoO_x−Ag/CeO_2-2	9.15	0.47	3.50
CoO_x−Ag/CeO_2-3	7.78	0.30	1.06
CoO_x−Ag/CeO_2-4	2.78	0.15	6.19

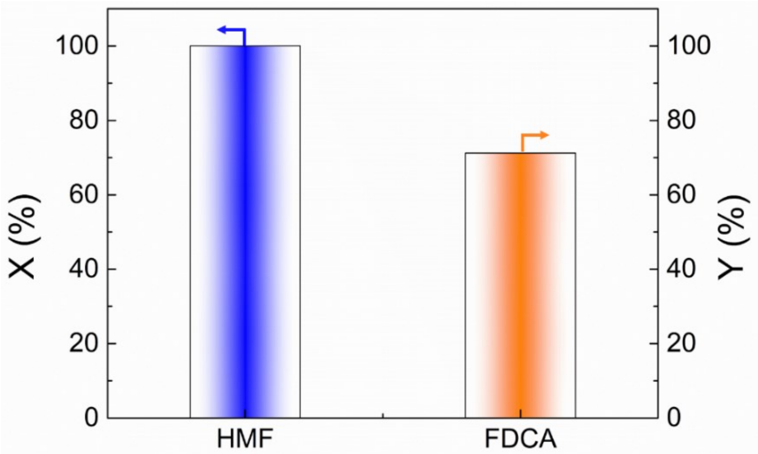

Fig. S7 HMF oxidation under base-free condition. Reaction conditions: HMF (0.05 mmol), catalyst (0.3 g), H_2O (20 mL), O_2 (2 MPa), 130 °C, 12 h.

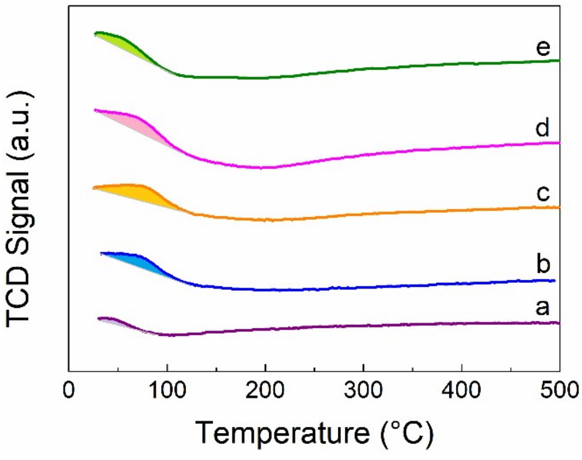

Fig. S8 O_2-TPO patterns of the catalysts. (a) Ag/CeO_2, (b) CoO_x−Ag/CeO_2-1, (c) CoO_x−Ag/CeO_2-2, (d) CoO_x−Ag/CeO_2-

3, (e) CoO_x–Ag/CeO_2-4.

Table S12 Oxygen Activation Capacity According to O_2-TPO Profiles.

Catalysts	OSC [μmol/g]
Ag/CeO_2	6.4
CoO_x–Ag/CeO_2-1	39.9
CoO_x–Ag/CeO_2-2	64.2
CoO_x–Ag/CeO_2-3	43.2
CoO_x–Ag/CeO_2-4	30.9

References

[1] G. D. Yadav and R. V. Sharma, *Appl. Catal. B.*, 2014, **147**, 293–301. DOI: 10.1016/j.apcatb.2013.09.004

[2] D. Zhao, D. Rodriguez-Padron, R. Luque and C. Len, *ACS Sustain. Chem. Eng.*, 2020, **8**, 8486–8495. DOI: 10.1021/acssuschemeng.9b07170

[3] O. R. Schade, K. F. Kalz, D. Neukum, W. Kleist and J. D. Grunwaldt, *Green Chem.*, 2018, **20**, 3530–3541. DOI: 10.1039/c8gc01340c

[4] O. R. Schade, F. Stein, S. Reichenberger, A. Gaur, E. Saraçi, S. Barcikowski and J. D. Grunwaldt, *Adv. Synth. Catal.*, 2020, **362**, 5681–5696. DOI: 10.1002/adsc.202001003

[5] J. An, G. Sun and H. Xia, *ACS Sustain. Chem. Eng.*, 2019, **7**, 6696–6706. DOI: 10.1021/acssuschemeng.8b05916

[6] B. L. Sang, J. Li, X. Q Tian, F. L. Yuan and Y. J Zhu, *Mol. Catal.*, 2019, **470**, 67-74. DOI: 10.1016/j.mcat.2019.03.026

[7] O. Casanova, S. Iborra and A. Corma, *ChemSusChem*, 2009, **2**, 1138 – 1144. DOI: 10.1002/cssc.200900137

[8] Q. Q. Li, H. Y. Wang, Z. P. Tian, Y. J. Weng, C. G. Wang, J. R. Ma, C. F. Zhu, W. Z. Li, Q. Y. Liu and L. L. Ma, *Catal. Sci. Technol.*, 2019, **9**, 1570-1580. DOI: 10.1039/ c9cy00211a

[9] Z. Z. Miao, Y. B. Zhang, X. Q. Pan, T. X. Wu, B. Zhang, J. W. Li, T. Yi, Z. D. Zhang and X. G. Yang, *Catal. Sci. Technol.*, 2015, **5**, 1314-1322. DOI: 10.1039/c4cy01060d

[10] C. Ferraz, M. Zielinski, M. Pietrowski, S. Heyte, F. Dumeignil, L. Marcia Rossi and R. Wojcieszak, *ACS Sustain. Chem. Eng.*, 2018, **6**, 16332–16340. DOI: 10.1021/acssuschemeng.8b03330

[11] C. Megías-Sayago, A. Lolli, S. Ivanova, S. Albonetti, F. Cavani and J. A. Odriozola, *Catal. Today*, 2019, **333**, 169-175. DOI: 10.1016/j.cattod.2018.04.024

[12] O. Schade, P. Dolcet, A. Nefedov, X. H. Huang, E. Saraçi, C. Wöll and J. Grunwaldt, *Catalysts*, 2020, **10**, 342-355. doi:10.3390/catal10030342

[13] N. K. Gupta, S. Nishimura, A. Takagaki and K. Ebitan, *Green Chem.*, 2011, **13**, 824–827. DOI: 10.1039/c0gc00911c

[14] C. Megías-Sayago, K. Chakarova, A. Penkova, A. Lolli, S. Ivanova, S. Albonetti, F. Cavani and J. Odriozola, *ACS Catal.*, 2018, 8, 11154−11164. DOI: 10.1021/acscatal.8b02522